Synchrotron-radiation soft-x-ray photoemission study of lead on $Bi_2CaSr_2Cu_2O_8$

H. Bernhoff, S. Söderholm, U. O. Karlsson, and S. A. Flodström
Materials Science, Department of Physics, KTH, S-100 44 Stockholm, Sweden

M. Qvarford, J. N. Andersen, R. Nyholm, and I. Lindau
MAX-lab, University of Lund, Box 118, S-221 00 Lund, Sweden
and Department of Synchrotron Radiation Research, Institute of Physics, Lund University, Sölvegatan 14, S-223 62 Lund, Sweden
(Received 26 November 1991; revised manuscript received 21 April 1992)

In this paper we present a study of the interaction of Pb with a clean single-crystal $Bi_2CaSr_2Cu_2O_8$ superconductor surface based on photoemission and low-energy electron diffraction (LEED). Deposition of Pb on a $Bi_2CaSr_2Cu_2O_8$ crystal kept at room temperature gives rise to the formation of metallic Bi and oxidized Pb at the interface. This behavior could not be observed when the crystal was kept at 100 K during Pb deposition. For all investigated Pb overlayers on a cold crystal (100 K), surface-sensitive photoelectron spectroscopy revealed the growth of a covering metallic Pb overlayer film. The growth at 100 K, contrary to the growth at room temperature, preserved the original LEED 5×1 pattern even for Pb depositions corresponding to a 24-Å thick overlayer indicating epitaxial growth. Furthermore, a rigid 0.4-eV shift of the valence band and the Bi $5d$ core levels is observed upon initial Pb deposition and is tentatively attributed to electron doping.

I. INTRODUCTION

The superconducting Bi-Ca-Sr-Cu-O system has since its discovery[1] been the subject of many elemental substitutions. The most successful improvement of the superconductor has been achieved by doping with Pb, which has proved to enhance the formation of the 110-K superconducting phase, known as the 2:2:2:3 phase.[2] In this paper we try to shed some light on the interaction of Pb with the $Bi_2CaSr_2Cu_2O_8$ structure. The fact that Pb is a low-temperature superconductor also contributes to the scientific interest of the interface. Furthermore, the $Bi_2CaSr_2Cu_2O_8$ system is specially suited for surface studies due to the availability of high-quality single crystals, the ease of cleavage, and the great surface stability under ultrahigh-vacuum (UHV) conditions.

II. EXPERIMENT

The single crystals used in this experiment were grown with a directional solidification method and are reported to show a sharp superconductive transition at 85 K.[3]

In all experiments the crystals were glued to the sample holders with a conducting UHV-compatible silver epoxy. The crystals were cleaved *in situ* and showed a smooth mirrorlike surface. Low-energy-electron-diffraction (LEED) gave the 5×1 pattern characteristic of the single-crystalline Bi-O surface.[4] All the LEED patterns were recorded with an incident-electron energy of 30 eV. In previous tests, which were performed on clean crystals, no degradation of the LEED pattern with time was observed, if the incident-electron energy was kept below 100 eV.

Pb was deposited from a tungsten-filament evaporation source, the flux being determined by a quartz-crystal monitor. Measurements were made on a clean surface and for successively increasing Pb overlayers up to 24 Å on a sample kept at room temperature (RT) and on a sample cooled to 100 K with corresponding Pb overlayers.

The photoelectron-spectroscopy experiments were performed at beamline 41 on the MAX-lab synchrotron-radiation source at Lund University, Sweden. This allowed photon energies in the range from 20 to 200 eV to be used in the experiments. The total resolution—photon and electron contributions—was determined, using the Fermi edge of gold, to be ≤ 0.25 eV. A description of the beamline can be found elsewhere.[5]

Complementary measurements on the clean crystal and the 1-Å-Pb-overlayered crystal at RT were made on beam-line 22. These measurements probed deeper core levels not accessible at beamline 41, mainly Sr $3d$. All the data presented in the figures of this work have been recorded at beamline 41. Beamline 22 offers photon energies from 20 to 1000 eV. As for beamline 41, a description can be found elsewhere.[6]

III. RESULTS AND DISCUSSION

Figure 1 shows LEED patterns for the clean crystal at RT [Fig. 1(a)] and for Pb overlayers of 12 and 24 Å deposited at 100 K [Figs. 1(b) and 1(c)]. The 5×1 LEED pattern of the clean crystal is maintained even for extensive Pb depositions, 12 and 24 Å, on the cold crystal, although the pattern is weaker and more diffuse. Although the spots in Figs. 1(b) and 1(c) are very weak due to poor photoreproduction the changes described here were clearly observed at the time of the experiment. Furthermore, the LEED patterns of Figs. 1(b) and 1(c) were maintained while moving the probe over the surface and varying the angle of incidence. Thus, the surface of the

Pb deposited on a cold crystal appears to maintain an ordered structure related to that of the cleaved $Bi_2CaSr_2Cu_2O_8$ crystal. Contrary to this behavior, LEED patterns monitored during successive deposition of Pb on the crystal at RT showed an abrupt degradation. After the deposition of 0.3 Å Pb the LEED pattern was already very weak and at 3 Å Pb it was completely lost.

Figure 2 shows photoelectron spectra of the Bi 5*d* and Pb 5*d* core-level regions, from the 100-K cooled crystal, irradiated with 100-eV photons. Both Figs. 2(a) and 2(b) display, starting from the bottom, spectra of the clean crystal, and consecutively thicker Pb overlayers towards the top. In Fig. 2(a) the normal-emission results are presented, while in Fig. 2(b) the spectra for the 60° emission are shown. In the latter case the probe is more surface sensitive due to the high emission angle. The spectra in Fig. 2, and also the other spectra in this work, are all normalized to the incoming photon flux.

The spectra recorded at 100 K are characteristic of an unreactive growth of a covering metallic Pb film. As the Pb coverage increases, a Pb 5*d* doublet, with a binding energy characteristic of metallic Pb, increases in intensity while the Bi 5*d* doublet fades. Additionally, the Bi 5*d* doublet shifts by about 0.4 eV to higher binding energy upon the initial 1-Å-Pb deposition, and stays at this higher binding energy upon subsequent Pb deposition. The origin of this shift will be discussed below.

The top spectra of Figs. 2(a) and 2(b), recorded after heating to RT, show a strongly reacted film. As a result of the annealing to RT, the Bi 5*d* doublet rises sharply to an intensity corresponding to that of the 6-Å-Pb RT covered crystal, while the intensity in the Pb region is redistributed. Besides the sharp metallic Pb 5*d* peak, a new doublet appears, shifted to a higher binding energy coinciding with that of oxidized Pb, implying a partial oxidation of the Pb.

When Pb is deposited at RT (Fig. 3), a much more complex behavior is observed. Besides the Bi 5*d* oxide doublet and the Pb 5*d* metallic peaks, the spectra also exhibit additional doublets corresponding to oxidized Pb and reduced Bi. At low coverage the Pb 5*d* doublet has binding energies of 19.70 and 22.35 eV, whereas at higher coverage an additional component appears with a binding energy equal to the metallic Pb 5*d* binding energy. The observed shift of 1.46 eV corresponds to that between metallic and oxidized Pb.[7,8] From the Pb 5*d* intensity variation as a function of Pb coverage and emission angle, it can be concluded that the oxidized Pb is situated at the interface. Furthermore, the appearance of yet another peak is observed. The binding energy of this peak is initially slightly below that of the Bi 5*d* doublet. As the coverage increases, this peak shifts to even lower binding energy, and for the 24-Å Pb coverage the shift corresponds to that between oxide Bi and metallic Bi.[9,10] This is more evident in Fig. 4, where the region discussed for some of the 60° emission spectra shown in Fig. 3(b) has been expanded. In the topmost (24 Å Pb) and the second-from-bottom (1 Å Pb) spectra of Fig. 4 it can be seen that the new peak is indeed a doublet. The surface-sensitive spectra of Fig. 3(b) as compared to normal-emission spectra in Fig. 3(a) also show that most of the metallic Bi resides at the surface, on top of the deposited Pb. The same behavior of reduced Bi has previously been reported for Cu overlayers on *in situ* cleaved $Bi_2CaSr_2Cu_2O_8$ crystals.[11] In the case of Cu this behavior could be directly attributed to the lower surface energy[12] of Bi (0.55 J/m^2) over that of Cu (1.85 J/m^2). Whereas the relation holds for Pb (0.61 J/m^2) and Bi, the difference is much smaller. A calculation performed according to the model of Miedema *et al.*[13,14] yields a Bi surface segregation consistent with the experimental data. The observed oxidation of Pb at the expense of a Bi

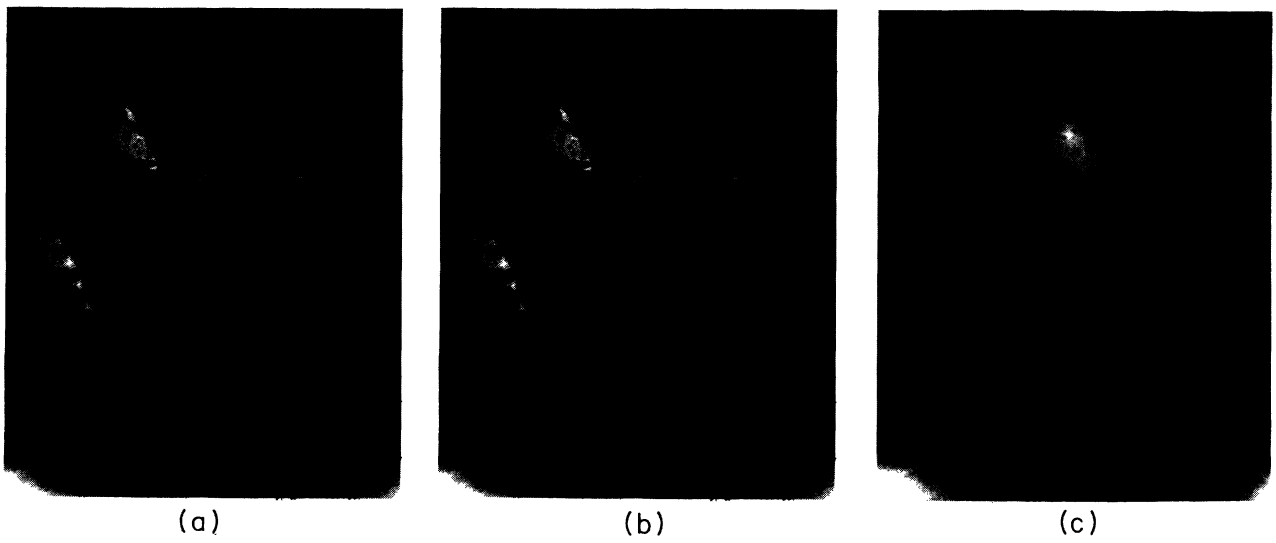

FIG. 1. LEED patterns of (a) clean $Bi_2CaSr_2Cu_2O_8$; (b) $Bi_2CaSr_2Cu_2O_8$ cooled to 100 K and covered with a 12-Å Pb overlayer; (c) same as (b), but covered with a 24-Å Pb overlayer.

reduction at the interface agrees with known data[15] on the heat of formation for PbO (218 kJ/mol) and BiO (211 kJ/mol). The small energy gain may explain why the reaction can be stopped by cooling to 100 K, i.e., by an activation barrier on the order of the thermal energy at RT. Finally, Fig. 3 reveals a shift of the Bi 5*d* oxide to higher binding energy analogous to the previously observed shift for Pb deposition at 100 K, which will be addressed below.

Figure 5 shows the ratio of metallic Pb 5*d* intensity to oxide Bi 5*d* intensity (from Figs. 2 and 3) for increasing Pb coverage as determined from fits with Doniach-Šunjić line shapes. The use of the intensity ratio eliminates possible errors due to normalization. The agreement of data points and the fitted exponential curve, shown as dashed lines and appropriate for the growth of a covering film, is very good for Pb growth on the cold crystal. Employing a simple cosine law of the obtained electron mean free paths for the cold crystal translates into an angle of 39° between normal emission and "60° emission." However, here we have neglected a number of effects on the angular distribution of photoelectron intensities, of which the most striking would be photoelectron diffraction. The points derived from the cold crystal after warming to RT fall far from the lines, indicating a strong reaction.

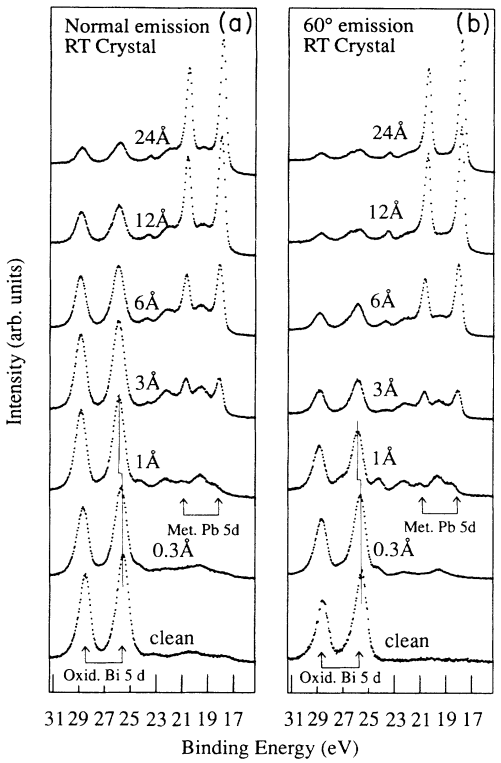

FIG. 3. Photoelectron spectra of the RT Pb-covered $Bi_2CaSr_2Cu_2O_8$ crystal Bi 5*d* and Pb 5*d* core-level region, irradiated with 100-eV photons; (a) normal emission and (b) 60° emission. From bottom to top: spectra of the clean crystal, then consecutively thicker Pb overlayers.

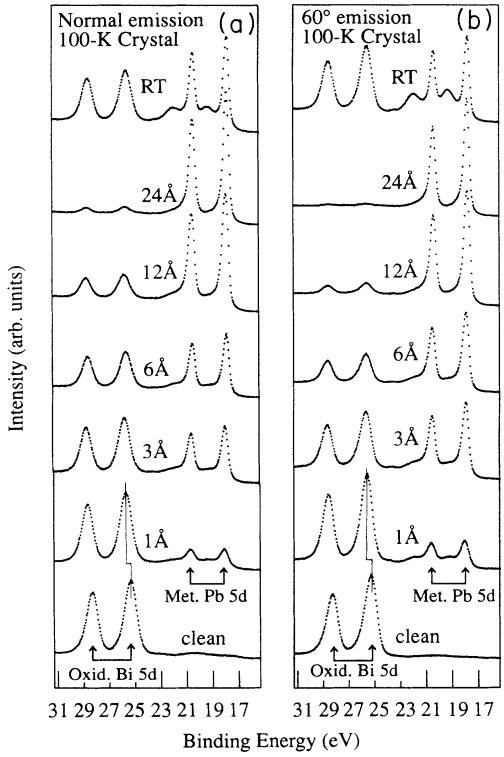

FIG. 2. Photoelectron spectra of the 100-K cooled $Bi_2CaSr_2Cu_2O_8$ crystal Bi 5*d* and Pb 5*d* core-level region, irradiated with 100-eV photons; (a) normal emission and (b) 60° emission. From bottom to top: spectra of the clean crystal, consecutively thicker Pb overlayers as indicated on the 100-K cooled crystal, and (on top) spectra after subsequent heating to RT.

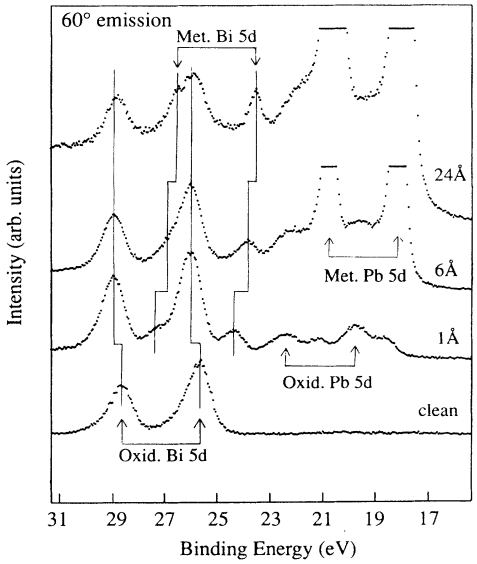

FIG. 4. An expansion of the critical Bi 5*d*–Pb 5*d* core-level region from Fig. 3(b) showing the growth of a metallic Bi 5*d* doublet, 60° emission, irradiated with 100-eV photons.

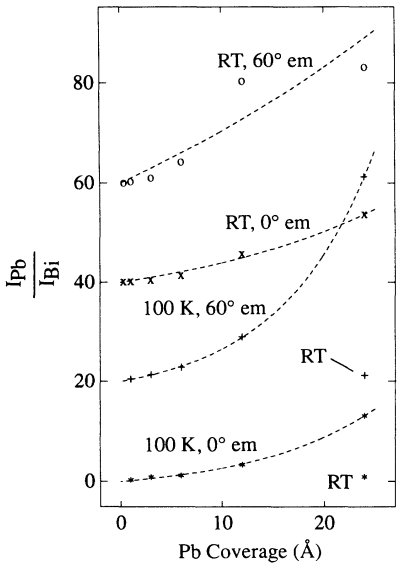

FIG. 5. The ratio of the metallic Pb peak intensity to the oxide Bi 5*d* intensity as a function of Pb coverage. Peak intensities are derived by a Doniach-Šunjić line-shape fit to the data presented in Figs. 2 and 3. From bottom to top: Pb growth on a 100-K cooled crystal, normal emission (*); 60° emission (+); Pb growth at RT, normal emission (×); RT, 60° emission (○). The intensities of the three upper data sets have been displaced by 20, 40, and 60 units, respectively.

In the case of the RT-grown Pb overlayer the best fits are not as good as for the Pb growth at 100 K, and lead to unphysical values for the electron mean free path in Pb.

The small metallic Bi peak revealed in the spectra of Figs. 3 and 4 has been studied in detail. In Fig. 6 the peak position is plotted as function of Pb-overlayer deposition for normal and 60° emission. Figure 6 distinguishes two distinct energy-shifted peaks, one at low Pb coverage, 24.2 eV, and one at higher Pb coverage, 23.5 eV, of which the latter agrees with values found in the literature for metallic Bi. We suggest that these components indeed originate from two different environments for the metallic Bi. The first shift, that in energy about halfway between that of oxidized and metallic Bi, is proposed to be derived from isolated Bi atoms on a Bi-O surface, and the latter from Bi atoms partly alloyed in a metallic Pb matrix and partly segregated to the Pb surface, as previously discussed.

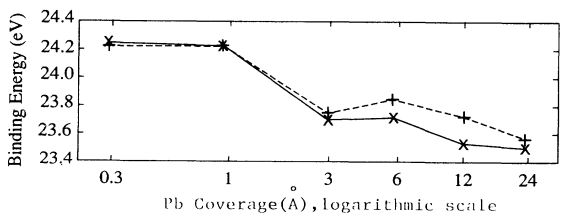

FIG. 6. The small metallic Bi peak position of Fig. 3 monitored as a function of Pb-overlayer deposition. The scale on the coverage axis is logarithmic. The two curves represent normal emission (dashed line) and 60° emission, (solid line), respectively.

Figure 7 shows the changes in the valence band upon Pb deposition for the cold and RT crystals, using a photon energy of 31 eV. The order of the spectra is reversed for clarity of presentation. Band-structure calculations suggest a valence-band region dominated by the strongly hybridized Cu 3*d*–O 2*p* band in the region 2–7 eV below the Fermi level and weaker Cu 3*d*–O 2*p* and Bi 6*p*–O 2*p* states[16] at the Fermi level. The clean-crystal spectrum, at the top of Fig. 7(a), shows the characteristic high density of states from 2 to 7 eV below the Fermi level, in good agreement with previously published results.[17] Spectra recorded at high Pb coverages on the 100 K crystal show much less intensity in this region, which is characteristic for metallic Pb.[18] As the Pb coverage increases, the cold crystal shows a rapid decrease in valence-band intensity, signifying a complete Pb coverage, while the RT-deposited Pb shows a more moderate decrease typical of the island growth mode. The behavior of the interface, as revealed by the valence-band spectra in Fig. 7 and discussed above, is in good agreement with what has been concluded from the behavior of the Bi and Pb core levels (Figs. 2 and 3).

One clear effect of Pb deposition seen in Fig. 7 is that the valence band shifts to higher binding energy for the initial depositions both at 100 K and at RT in the same

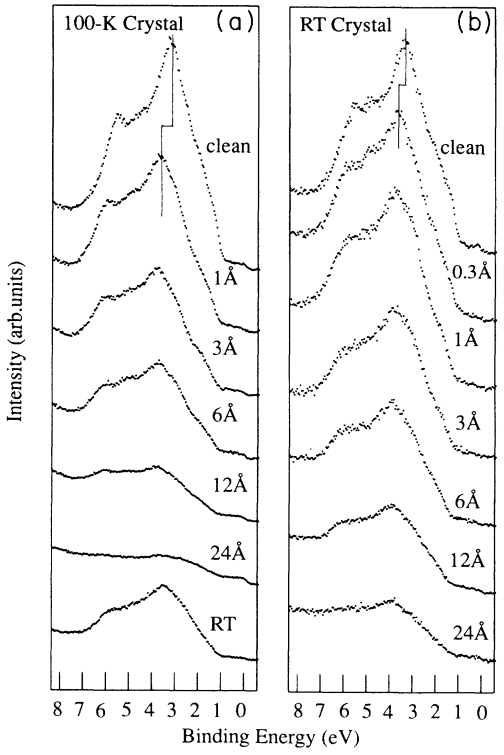

FIG. 7. Normal-emission valence-band spectra of (a) cold $Bi_2CaSr_2Cu_2O_8$ and (b) RT crystals for increasing Pb overlayers, using a photon energy of 31 eV. The order of the spectra is, for clarity of presentation, the reverse of that of Figs. 2 and 3. The bottom spectrum of Fig. 6(a) shows the 24-Å-Pb-covered crystal after subsequent heating to RT.

way as the Bi 5*d* core levels shift. The shift of the valence band has previously been reported for Pb deposition on polycrystalline $Bi_2CaSr_2Cu_2O_8$ (Ref. 19) and was suggested to stem from a disruption of Bi-O and Cu-O bonds. However, our core-level data in Fig. 2 show that the Bi-O surface is quite inert for Pb deposition at 100 K, indicating that this explanation is doubtful. Instead, the shift of the valence band and Bi 5*d* core level is assigned to doping, i.e., a shift of the chemical potential. Hall-effect measurements give 3.7 charge carriers per unit cell.[20] This number is in agreement with the concentration obtained from the measurements of the plasma frequency.[21,22] The deposition of 1 Å of Pb corresponds to 0.3 injected charge carriers per unit cell, assuming a Pb valence of 1+. This number can explain the observed shifts in both of the common models of high-temperature superconductors, namely the one-electron picture and the doped charge-transfer insulator model. In one-electron theory a charge transfer of 0.2 occurs[23] from Bi-O to Cu-O_2 in $Bi_2CaSr_2Cu_2O_8$, a number of the same magnitude as the number of injected carriers from the deposited Pb. In the doped charge-transfer model an impurity band, due to doping, gives rise to a finite density of states at the Fermi level. In this picture fairly small changes of the number of charge carriers can induce large changes of the chemical potential and/or band filling since such an impurity band is expected to be narrow. A chemical-potential shift of Bi 5*d* core levels and the valence band as a function of doping has been reported by Shen *et al.*[24] The doping was controlled by varying the oxygen concentration. The authors report a shift of 0.15–0.2 eV to lower binding energy upon hole doping. This is in good agreement with the observed shift of 0.4 eV to higher binding energies upon electron doping.

The bottomost spectrum of Fig. 7(a) exhibits a striking reaction where the 24-Å-Pb-deposited film seems to be be strongly reacted upon heating to RT. Comparing this valence-band spectrum to the spectra of the RT-deposited Pb overlayer, Fig. 7(b), suggests a remaining metallic Pb layer, after warming to RT, in the range of 12 Å. The intensities of the core-level peaks (Fig. 2) signify, in the same way, a remaining metallic Pb overlayer in the range of 6 Å Pb. Thus the deposition at low temperature followed by a slow heating to RT appears to be more destructive to the Pb film than a deposition at RT. This is believed to be caused by the oxidation of the Pb at the Bi-O interface layer, which certainly would upset the top Pb metallic film.

The valence-band spectra in Fig. 7(b) of the RT-grown Pb film, do not reveal any significant changes besides the effects on the states just below the Fermi level, which will be discussed in detail later, and the shift discussed previously. In fact, this lack of change in the valence-band spectra implies that the Cu-O_2 layers are relatively unaffected by deposition of Pb on the Bi-O surface.

In the 31-eV photon-energy spectra a fairly weak density of states at the Fermi level is observed. However, the states around the Fermi level are seen more clearly in the spectra recorded with a photon energy of 100 eV, shown in Fig. 8. The order of the spectra is the same as in Figs. 2 and 3, i.e., the spectrum of the clean crystal at the bottom and consecutively higher Pb coverage towards the top. The cold and the RT-deposited Pb overlayers show a rather different behavior. In the case of the former very little happens upon deposition of the first Pb layer and at higher coverages the rise of a sharp metalliclike Fermi edge is observed. Upon warming of the cold crystal to RT the originally sharp metalliclike Fermi edge is reduced. In the case of the RT-deposited Pb, a marked reduction of the density of states at the Fermi level occurs. A metalliclike Fermi edge is only observed for the 24-Å-Pb-covered crystal and is not at all as sharp as that of the cold crystal. This behavior lends further support to the inferred disruption of the Bi-O layer in RT Pb growth. The notion of a disruption of the Bi-O layer is consistent with the remnant intensity at the Fermi level in Fig. 8(b), since this intensity could be attributed to states in the Cu-O_2 layer, which, as discussed, seems to be relatively undisturbed by the reaction at the Bi-O layer.

For the cold crystal, the observed LEED patterns combined with the strong evidence for the growth of a completely covering film of Fig. 5, as opposed to island or a Stransky-Krastanov microstructure, supports the adoption of an epitaxial-growth model. However, the assumption of an epitaxial growth of Pb on the cold crystal appears somewhat doubtful since a $(1/\sqrt{2}\times 1/\sqrt{2})R45°$ Pb growth on Bi, O, or interstitial positions would give a substrate lattice parameter of 3.8 Å ($5.4/\sqrt{2}$ Å). Com-

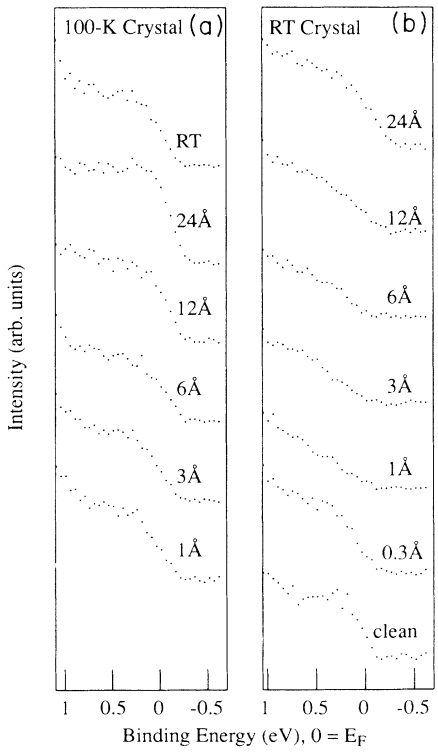

FIG. 8. Spectra of the Fermi-level region for increasing Pb overlayers on (a) the 100-K cooled crystal and (b) the RT crystal. Spectra of the clean crystal are at the bottom right and those of consecutively higher Pb coverage are towards the top of the figure; the RT warmed crystal spectrum is at the top of the cold crystal spectra in the left part of the figure.

paring this to the nearest-neighbor distance of metallic lead, which is 3.5 Å, gives a lattice mismatch of 8.5%. It could be argued that an overlayer film consisting of an alloy of Pb with the metallic Bi would have a larger lattice parameter. Although it has been shown that Bi expands the lattice of Pb,[25] the maximum expansion is only 0.5%. It could also be speculated that the softness of the Pb and, even more, that of the Pb-Bi alloy makes the 8.5% stretching feasible. What further complicates the situation is the presence of the $Bi_2CaSr_2Cu_2O_8$ superstructure, giving rise to the observed and maintained 5×1 LEED pattern. Different origins have been suggested: a missing row of Bi atoms,[26] extra oxygen in Bi-O layers,[27] or a buckling of the entire $Bi_2CaSr_2Cu_2O_8$ structure.[28] Regardless of the reason for the superstructure, it is clear that the situation is more intricate than a simple lattice mismatch of 8.5%. It could, for example, be speculated that the missing row would compensate for most of the lattice mismatch or that a buckling would allow the growth of a consecutively less buckled Pb overlayer, which would thereby be relaxed. As the present data are not conclusive in this respect, we limit our conclusion to note that the data indicate the growth of a strained epitaxial Pb overlayer.

The strain in the Pb overlayer, induced by the proposed stretching, would most likely contribute to the observed disruption of the Pb overlayer upon heating to RT. It is also interesting to compare the present result to those of Hwu *et al.*[29] who deals with the Pb:Y-Ba-Cu-O interface in the 50-K range. The authors conclude that the "Pb overlayer thickness is close to that of a layer-by-layer growth on a smooth surface," although they worked on sintered samples and not single crystals.

Another issue of interest concerns the interaction of Pb with the Sr-O, $Cu-O_2$, and Ca layers of the $Bi_2CaSr_2Cu_2O_8$ system. It is important to remember that the measurements have been made on cleaved single crystals, which, from the surface and down, consist of Bi-O, Sr-O, $Cu-O_2$, Ca, and then the oxides repeated in reverse order. This means that the deposited Pb first encounters Bi-O. The Sr 3*d* core-level region, probed at beamline 22 with 250-eV photon energy, not presented here, showed no signs of reaction for a 1-Å-Pb overlayer. This suggests a reaction of Pb with Bi-O on top of an inert Sr-O layer. The Sr-O layer has a very high heat of formation (596 kJ/mol) and was shown earlier to be very stable against reactions with an overlayer metallic film.[11]

IV. SUMMARY AND CONCLUSION

When the Pb:$Bi_2CaSr_2Cu_2O_8$ interface is formed at RT, a thin layer of Pb oxide is formed at the interface and small amounts of Bi are reduced to metallic Bi. The reduction is in agreement with known data[15] on heat of formation for PbO (218 kJ/mol) and BiO (211 kJ/mol), although the energy gain is small. The reduced Bi appears to segregate to the Pb surface, while the oxidized Pb stays at the interface. The very same experiment on crystals kept at 100 K shows no sign of these reactions. However, after the cold crystal has been warmed to RT, a reaction was observed, indicating an activation energy for the reduction of the Bi by Pb at the $Bi_2CaSr_2Cu_2O_8$ surface on the order of the thermal energy at RT. The RT-grown interface is not as sharp as the 100-K-grown interface since a metalliclike Fermi edge appears only for the 24-Å-thick overlayers. Moreover, the RT Pb overlayer exhibits an island growth, while Pb on the 100-K cooled crystal appears to grow as a strained epitaxial covering film. The observed 0.4-eV shift of Bi 5*d* and the valence band to higher binding energy is attributed to doping effects rather than chemical reactions involving the Bi-O surface.

ACKNOWLEDGMENTS

We thank Dr. Z.-X. Shen for providing the single crystals and for useful discussions. This work was supported by the Swedish Natural Science Research Council and the Swedish National Board for Technical Development.

[1]H. Maeda, Y. Tanaka, M. Fukutomi, and T. Asano, Jpn. J. Appl. Phys. **27**, L209 (1988).
[2]D. Shi, M. S. Boley, J. G. Chen, M. Xu, and A. Zangvil, Appl. Phys. Lett. **55**, 699 (1989).
[3]D. B. Mitzi, L. W. Lombardo, A. Kapitulnik, S. S. Laderman, and R. D. Jacowitz, Phys. Rev. B **41**, 6564 (1990).
[4]P. A. P. Lindberg, Z.-X. Shen, B. O. Wells, D. B. Mitzi, I. Lindau, W. E. Spicer, and A. Kapitulnik, Appl. Phys. Lett. **53**, 2563 (1988).
[5]U. O. Karlsson, J. N. Andersen, K. Hansen, and R. Nyholm, Nucl. Instrum. Methods A **282**, 553 (1989).
[6]J. N. Andersen, O. Björneholm, A. Sandell, R. Nyholm, J. Forsell, L. Thånell, A. Nilsson, and N. Mårtensson, Sync. Rad. News **4**, 15 (1991).
[7]K. S. Kim, T. J. O'Leary, and N. Winograd, Anal. Chem. **45**, 2214 (1973).
[8]S. Evans and J. M. Thomas, J. Chem. Soc. Faraday Trans. II **70**, 313 (1974).
[9]R. Nyholm, A. Berndtsson, and N. Mårtensson, J. Phys. C **13**, L1091 (1980).
[10]Y. Schuhl, H. Baussart, R. Delobel, M. Le Bras, J. Leroy, L. Gengembre, and J. Grimblot, J. Chem. Soc. Faraday Trans. I **79**, 2055 (1983).
[11]H. Bernhoff, M. Qvarford, S. Söderholm, A. S. Flodström, J. N. Andersen, R. Nyholm, U. O. Karlsson, and I. Lindau, Physica C **180**, 120 (1991).
[12]A. R. Miedema, Z. Metallkd. **69**, 287 (1978).
[13]A. R. Miedema, Z. Metallkd. **69**, 455 (1978).
[14]A. R. Miedema, F. R. deBoer, R. Boom, and J. W. F. Dorleijn, CALPHAD **341**, 1 (1977).
[15]*Handbook of Chemistry and Physics,* 56th ed., edited by R. C. Weast (Chemical Rubber Co., Cleveland, 1975), pp. D45–D50.
[16]H. Krauker and W. E. Pickett, Phys. Rev. Lett. **60**, 1665 (1988).
[17]T. Takahashi, H. Matsuyama, H. Katayama-Yoshida, Y. Ok-

abe, S. Hosoya, K. Seki, H. Fujimoto, M. Sato, and H. Inokuchi, Nature (London) **334**, 691 (1988).
[18]J. J. Yeh and I. Lindau, At. Data Nucl. Data Tables **32**, 1 (1985).
[19]P. Kulkarni, S. Mahamuni, S. K. Kulkarni, and S. Nigavekar, Physica C **168**, 104 (1990).
[20]A. Maeda, H. Hase, I. Tsukada, K. Noda, S. Takebayashi, and K. Uchinokura, Phys. Rev. B **41**, 6418 (1990).
[21]Y.-Y. Wang, G. Feng, and A. L. Ritter, Phys. Rev. B **42**, 420 (1990).
[22]K. Hirochi, K. Mizuno, T. Matsushima, Y. Ichikawa, S. Hayashi, H. Adachi, K. Setsune, and K. Wasa, Jpn. J. Appl. Phys. **29**, L1104 (1990).
[23]M. S. Hybertsen and L. F. Mattheiss, Phys. Rev. Lett. **60**, 1661 (1988).
[24]Z.-X. Shen, D. S. Dessau, B. O. Wells, C. G. Olson, D. B. Mitzi, L. Lombado, R. S. List, and A. J. Arko, Phys. Rev. B **44**, 12 098 (1991).
[25]C. Tyzack and G. V. Raynor, Scr. Cryst. **7**, 505 (1954).
[26]M. D. Kirk, J. Nogami, A. A. Baski, D. B. Mitzi, A. Kapitulnik, T. H. Geballe, and C. F. Quate, Science **242**, 1673 (1988).
[27]H. W. Zandbergen, W. A. Groen, F. C. Mijlhoff, and G. van Tendeloo, Physica C **156**, 325 (1988).
[28]C. K. Shi, R. M. Feenstra, J. R. Kirtley, and G. V. Chandrashekhar, Phys. Rev. B **40**, 2682 (1989).
[29]Y. Hwu, C. Hwang, R. T. Wu, M. Marsi, M. Onellion, G. Margaritondo, and D. E. Morris, Solid State Commun. **76**, 349 (1990).

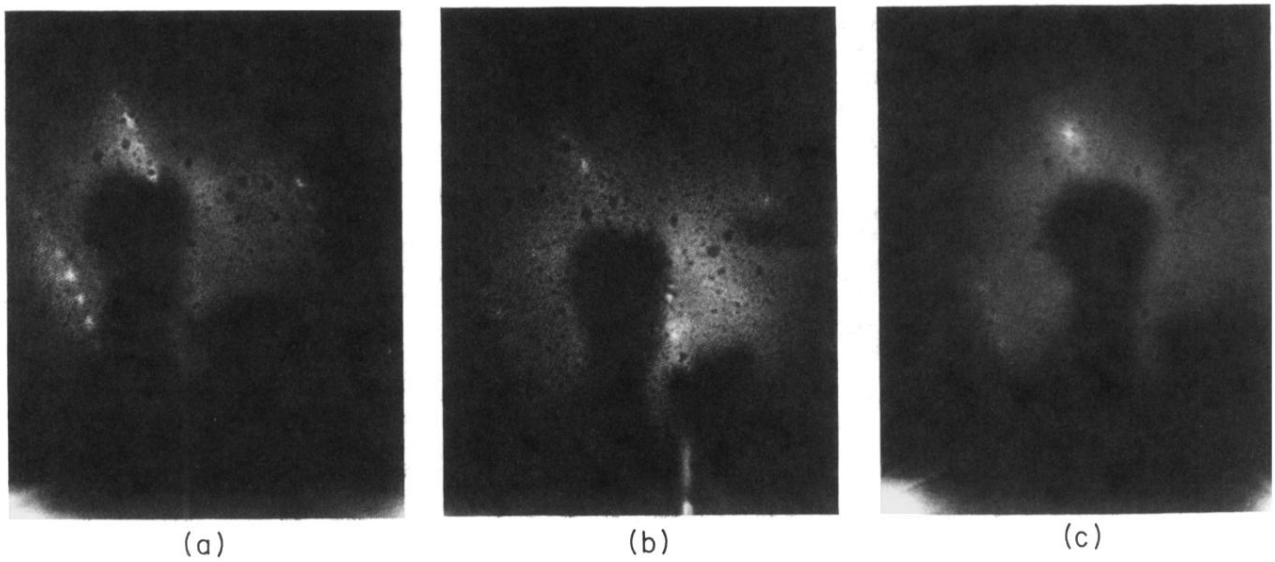

FIG. 1. LEED patterns of (a) clean $Bi_2CaSr_2Cu_2O_8$; (b) $Bi_2CaSr_2Cu_2O_8$ cooled to 100 K and covered with a 12-Å Pb overlayer; (c) same as (b), but covered with a 24-Å Pb overlayer.